two-term solution yields a fundamental frequency value which is in very good agreement with the one obtained in Refs. 6 and 7 (even the result obtained by means of a one-term solution possesses good engineering accuracy).

Table 2 presents values of Ω_0 for the linearly tapered beam ($\alpha=\beta=1.2$) rigidly clamped ($\phi'=0$) for various axial force parameters and mass ratios $\nu=M/M_v$. For $\nu=0$ the results are in good agreement with the frequency values available in the open literature.[8]

Table 3 contains values of Ω_0 in the case of a structural element with discontinuously varying cross section.

Judging from the accuracy attained in those cases where exact values are available, it seems that the present approach yields useful results when an engineering answer is needed. An inherent advantage of the methodology is the fact that it can be easily implemented on a desk computer.

Acknowledgment

The present investigation has been partially sponsored by Comisión de Investigaciones Cientificas (Buenos Aires Province).

References

[1]Wagner, H. and Ramamurti, V., "Beam Vibrations—A Review," *The Shock and Vibration Digest,* Vol. 9, No. 9, 1977, pp. 17-24.

[2]Sato, K., "Transverse Vibrations of Linearly Tapered Beams with Ends Restrained Elastically Against Rotation Subjected to Axial Force," *International Journal of Mechanical Sciences,* Vol. 22, No. 2, 1980, pp. 109-115.

[3]Housner, G. W. and Keightley, W. O., "Vibrations of Linearly Tapered Cantilever Beams," *Journal of Engineering of the Mechanics Division,* ASCE, Vol. 128, Pt. I, 1963, pp. 1020-1054.

[4]Laura, P. A. A., Pombo, J. L., and Susemihl, E. A., "A Note on the Vibrations of a Clamped-Free Beam with a Mass at the Free End," *Journal of Sound and Vibration,* Vol. 37, No. 2, 1974, pp. 161-168.

[5]Timoshenko, S. P. and Gere, J. M., *Theory of Elastic Stability,* 2nd ed., McGraw Hill Book Co., New York.

[6]Gutiérrez, R. H. and Laura, P. A. A., "Coupled Flexural-Torsional Vibrations of a Beam Elastically Restrained at One End and Carrying a Concentrated Mass at the Other," *Journal of Sound and Vibration,* Vol. 58, No. 2, 1978, pp. 305-309.

[7]Blevins, R. D., *Formulas for Natural Frequency and Mode Shape,* Van Nostrand Reinhold Company, New York, 1979, p. 163.

[8]Mabie, H. H. and Rogers, C. B., "Transverse Vibrations of Tapered Cantilever Beams," *Journal of the Acoustical Society of America,* Vol. 51, April 1972, pp. 1771-1774.

Parameters for the Simulation of High Temperature Blown Shock Layers

R. N. Gupta*

NASA Langley Research Center, Hampton, Virginia

Introduction

FOR the Galileo mission to Jupiter, the massive-ablation injection rates (from the probe's forebody heat shield) driven by radiative heating from the high-energy shock-layer gases create a unique flowfield environment.[1] Such an environment is very difficult to simulate in a ground-based experimental facility. Since all conditions can not be duplicated, care must be taken in what quantities are simulated in an experiment. Holden's[2] recent work is one of the few experiments applicable to the problem. In this study, he attempted to duplicate a few of the aspects of the entry environment for the stagnation region of the Galileo probe. This work presented many interesting results on the structure and stability of the shock layer over a hemispherical nose-tip body at blowing rates of $0<\rho_w v_w/\rho_\infty u_\infty<0.7$ using CF_4 as the principal injectant. Here, ρ_w and ρ_∞ are the wall and freestream values of the density, v_w is the normal injection velocity at the wall, and u_∞ is the freestream velocity. The interpretation of Holden's results, however, requires an analysis of the important parameters in a massively blown reentry flowfield. The present study explores the impact of the ratios of injection-to-freestream velocity (v_w/u_∞), wall-to-freestream density (ρ_w/ρ_∞), and the shock-layer to ablation-layer gas temperature (T_s/T_w) in simulating the high-temperature blown shock layers. The roles played by these ratios are considered quite important. For example, a larger value of the injection velocity for a given injection rate implies a greater boundary-layer thickness. This, in turn, would entrain more of the high-temperature, radiating gases in the outer portions of the shock layer. These gases would be brought into the lower regions of the shock layer by turbulent diffusion, resulting in higher temperatures close to the body surface for a prescribed surface temperature. Similarly, using a smaller outer shock layer to wall temperature ratio (T_s/T_w) would affect the boundary-layer thickness and entrainment rate.

The purpose of this Note is to evaluate the importance of the velocity, density, and temperature ratios outlined in the previous paragraph. In order to keep the analysis simple, only perfect-gas results for a hydrogen-helium atmosphere are obtained here.

Analysis

For the purpose of analysis, the time-dependent viscous-shock-layer equations of motion[3] for a perfect-gas mixture for turbulent flow have been considered. With these equations no-slip boundary conditions are used at the surface and the wall temperature is assigned a constant value. The surface mass injection rate is specified either as a constant value or varied according to the distribution of Fig. 1. The boundary conditions at the shock are calculated by using the shock relations. A two-layer eddy-viscosity model[4] consisting of an inner law based upon Prandtl's mixing length concept and the Clauser-Klebanoff expression for the outer law is used in the present investigation.

The solutions to the governing equations have been obtained by a time-asymptotic two-step finite-difference method due to MacCormack.[5] The details of the vectorized code are given in Ref. 6 and the results have been obtained on the CYBER 203 computer.

Results and Conclusions

As pointed out in the Introduction, the primary purpose of this study is to evaluate the importance of velocity (v_w/u_∞), density (ρ_w/ρ_∞), and shock-layer to ablation-layer gas temperature (T_s/T_w) ratios for the simulation of high-energy blown shock layers. In particular, the role played by these parameters is studied as to their influence on the entrainment of high-temperature outer region gases since this significantly changes the chemical composition and temperature distribution through the shock layer and, in turn, controls the transport of radiative energy to the probe surface.

In this study, attention has been focussed on the spherical portion of the probe. In order to obtain results over a large part of the curved surface, the probe shape with a small half-angle as shown in Fig. 2 has been studied. (Nomenclature used

---

Received Jan. 11, 1982; revision received May 26, 1982. This paper is declared a work of the U.S. Government and therefore is in the public domain.

*NRC—Senior Research Associate, Aerothermodynamics Branch, Space Systems Division, on leave from IIT, Kanpur, India; Professor, Department of Aeronautical Engineering. Member AIAA.

in Fig. 2 and subsequently follows that of Ref. 3. The quantities with an asterisk denote dimensional values.) The freestream conditions and other parameters employed in the analysis have been taken from Ref. 2 and are as follows.

$M_\infty = 12$
$r_N^* = 0.1524$ m
$Re = \rho_\infty^* u_\infty^* r_N^* / \mu_\infty^* = 2.8 \times 10^6$
$\rho_\infty^* = 6.267 \times 10^{-3}$ kg/m^3
$\mu_\infty^* = 1.324 \times 10^{-6}$ Ns/m^2
$Pr = 0.72$
R^*(gas constant) = 3464.292 J/kg K
Gas mixture: $0.80H_2 + 0.20He$ under perfect-gas assumption
$T_w^* = 300$ K
$T_\infty^* = 20.85$ K
$\gamma = 1.4$ [Note that the value of γ would be a little higher for the gas mixture considered here at $M_\infty = 12$. For the actual Jovian entry condition (which occurs at a very high Mach number), however, the value of γ to be employed in a perfect-gas analysis would be lower than 1.4 to simulate the correct shock standoff distance.]

It may be mentioned that no direct comparison with the measurements of Ref. 2 is intended here. Even though the conditions of Ref. 2 are not far from the perfect-gas flowfield assumption as used presently, the mass diffusion of the injectants such as CF_4 and N_2 into the $H_2 + He$ shock layer has not been accounted for adequately in the present analysis, except through the density differentials obtained from the employment of different wall temperatures. The relevance of the present work, however, lies in the fact that it qualitatively brings out the importance of certain parameters (pointed out in the Introduction) for the simulation of high-temperature blown shock layers and helps in the interpretation of results of Ref. 2 for application to the Jovian entry environment. For example, in the experiments of Ref. 2, the injection-to-freestream velocity (v_w/u_∞) and wall-to-freestream density (ρ_w/ρ_∞) ratios were varied from about 0.009 and 565 for CF_4 to 0.0023 and 218 for N_2, respectively, for an injection rate ($\dot{m}_0$) of 0.5 at the stagnation point. For the 310-kg probe under peak-heating condition, however, the values of these velocity and density ratios are[3] about 0.004 and 1315, respectively, at the stagnation point for $\dot{m}_0 \approx 0.53$. Further, the ratio of shock-layer to ablation-layer gas temperatures is about 4 as compared to the ratio of about 2 considered in Ref. 2. The roles played by the velocity, density, and the temperature ratios listed here are considered quite important in the simulation of high-energy entry flowfields. The subsequent discussion qualitatively establishes these roles.

In order to simulate the entrainment rates corresponding to heavier and lighter injectant gases, the calculations have also been carried out for wall temperatures of 150 and 600 K, respectively, in addition to a wall temperature of 300 K listed earlier. These calculations further point out the role played by the density ratio, ρ_w/ρ_∞. For example, the density ratio at 600 K would be smaller by a factor of 2 when compared to the one at 300 K. For a given injection rate ($\dot{m}$), this would have the effect of doubling the injection-velocity ratio v_w/u_∞ and, thus, increasing the entrainment rate. Some calculations have also been performed at $M_\infty = 17$. This value of the Mach number gives a value of 4 for the shock-layer-to-wall temperature ratio (T_s/T_w). This ratio has a value of about 2 at $M_\infty = 12$. At $M_\infty = 17$, the only other variation in the values of the flowfield parameters given earlier is $Re = 3.94 \times 10^6$. The various computed results are displayed in Figs. 3 and 4.

Figure 3 shows the variations in the normal velocity, temperature, and eddy-viscosity profiles for different values

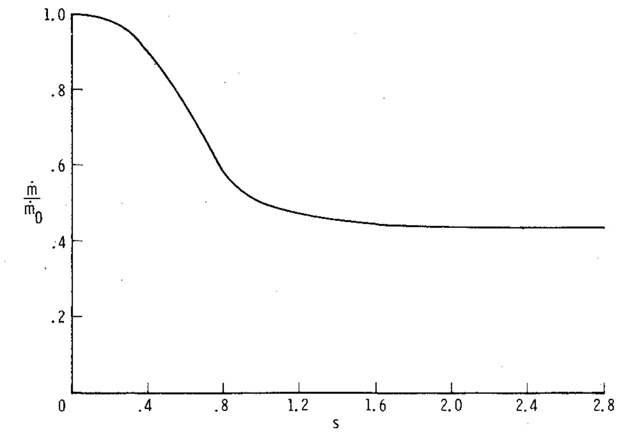

Fig. 1 Surface mass injection distribution for predicted Jupiter entry (taken from Ref. 2).

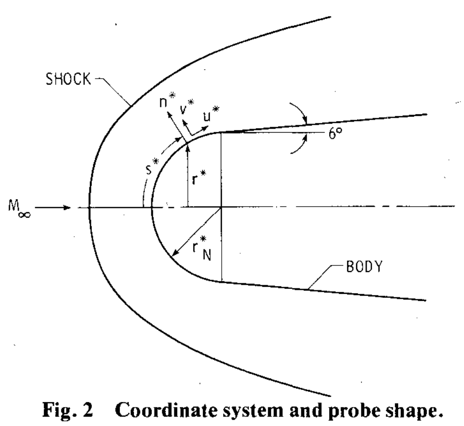

Fig. 2 Coordinate system and probe shape.

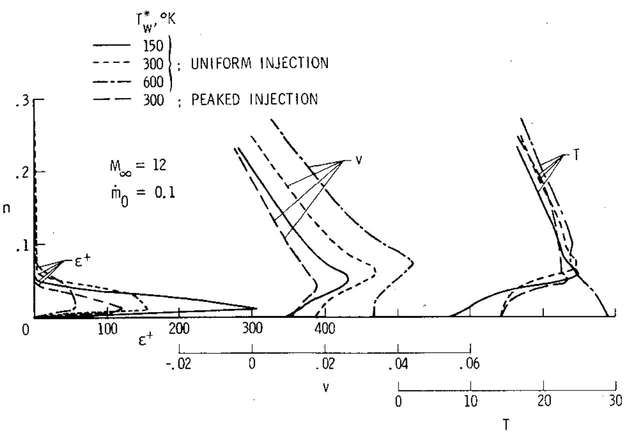

Fig. 3 Variation of the eddy viscosity, normal velocity, and temperature profiles with different wall temperatures at $s = 0.916$.

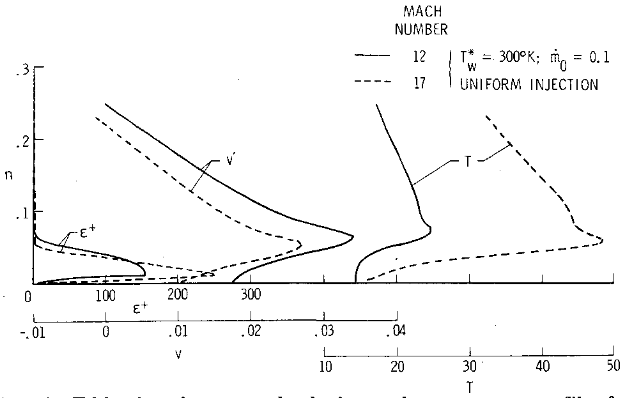

Fig. 4 Eddy viscosity, normal velocity, and temperature profiles for $M_\infty = 12$ and 17 at $s = 0.916$.

of the wall temperatures at $M_\infty = 12$. For a perfect gas, these temperature values simulate light-to-heavy gas injection at the surface. It is seen from the normal velocity profiles that the boundary-layer thickness would be larger with a lighter gas injection (or, equivalently, with a smaller density ratio at the wall). With the larger boundary-layer thickness, more of the outer region high-temperature shock-layer gases are entrained and brought into the lower region by turbulent diffusion. This changes the temperature distribution through the shock layer significantly, making the profiles fuller as compared to the case with a heavier gas injection. This, for actual entry conditions, affects the transport of radiative energy to the probe surface. It may be mentioned here that, due to the simulation of heavy-to-light gas injection through the specification of different wall temperatures for a perfect gas, the flow region near the wall is dominated by the specified wall-temperature value. With the peaked surface injection, the entrainment rates are smaller, the blown shock layer is closer to the surface, and the maximum temperature in the shock layer is also smaller as compared to the uniform injection case. The results presented are for the surface injection rate ($\dot{m}_0$) of 0.1 at the axis of symmetry. The normalized eddy-viscosity profiles of Fig. 3 also exhibit a character consistent with the normal velocity and temperature profiles. The maximum values of the eddy viscosity in the shock layer are larger for smaller entrainment rates due to poor turbulent diffusion.

Figure 4 contains results obtained for $M_\infty = 17$, $T_w^* = 300$ K, and uniform surface injection rate. These are compared with the corresponding results for $M_\infty = 12$ at the same body station ($s = 0.916$) located at 52.5 deg from the stagnation line. The normal velocity profiles suggest that, for a given value of the surface-injection rate, there is a larger entrainment of the shock-layer gases at the lower Mach number. This results in larger mixing due to turbulent diffusion. The temperature and eddy-viscosity profiles also show smaller gradients associated with larger mixing for the smaller Mach number.

It is clear from the current results that injection mass flow rate alone is not an adequate parameter to model the effects of massive blowing. For a prescribed injection rate, the wall-to-freestream density ratio (reflected through the wall-to-freestream temperature ratio), the injection velocity ratio, and the shock-layer-to-wall temperature ratio play important roles in establishing the entrainment of shock-layer gases. These, in turn, specify the mixing by turbulent diffusion and temperature levels through the shock layer. Thus, through the employment of nonrepresentative values of these parameters, wrong chemical composition and temperature distributions may be obtained and the transport of radiative energy to the surface could be simulated wrongly for the actual probe.

References

[1] Moss, J. N., "A Study of the Aerothermal Entry Environment for the Galileo Probe," AIAA Paper 79-1081, Orlando, Fla., June 1979.

[2] Holden, M. S., "An Experimental Study of Massive Blowing from a Nosetip During Jovian Entry," AIAA Paper 81-1070, Palo Alto, Calif., June 1981.

[3] Moss, J. N. and Kumar, A., "Significance of Turbulence and Transition Location on Radiative Heading with Ablation Injection," AIAA Paper 81-0281, St. Louis, Mo., Jan. 1981.

[4] Anderson, E. C. and Moss, J. N., "Numerical Solution of the Hypersonic Viscous-Shock-Layer Equations for Laminar, Transitional, and Turbulent Flows of a Perfect Gas Over Blunt Axially Symmetric Bodies," NASA TN D-7865, Feb. 1975.

[5] MacCormack, R. W., "The Effect of Viscosity in Hypervelocity Impact Cratering," AIAA Paper 69-354, Cincinnati, Ohio, April 1969.

[6] Kumar, A. and Graves, R. A. Jr., "A Vectorized Code for Calculating Laminar and Turbulent Hypersonic Flows about Blunt Axisymmetric Bodies at Zero and Small Angles of Attack," NASA TM 80202, Jan. 1980.